Electronic Supplementary Material (ESI) for ChemComm.

Supporting Information

Sustainable cycling enabled by high-concentration electrolyte for lithium-organic batteries

Ying Huang [ac], *Chun Fang* [b]*, *Wang Zhang* [b], *Qingju Liu* [a]*, *Yunhui Huang* [bc]*

[a] *School of Physics and Astronomy, School of Materials Science and Engineering, Yunnan Key Laboratory for Micro/Nano Materials & Technology, Yunnan University, Kunming 650091, PR China*

[b] *State Key Laboratory of Material Processing and Die & Mould Technology, School of Materials Science and Engineering, Huazhong University of Science and Technology, Wuhan 430074, PR China*

[c] *Collaborative Innovation Center of Intelligent New Energy Vehicle School of Materials Science and Engineering, Tongji University, Shanghai 201804, PR China*

Corresponding authors:

E-mail: fangchun@hust.edu.cn, qjliu@ynu.edu.cn, huangyh@tongji.edu.cn

Experimental Section

Synthesis of CuTCNQ/CNFs composite. The precursor solution is consisting of 1 g polyacrylonitrile (PAN), 0.5 g copper acetate ($Cu(OAc)_2$) and 10 mL N, N-dimethylformamide. The solution was used to prepare freestanding nanofibers film by electrospinning. The $Cu(OAc)_2$/PAN nanofibers were stabilized at 280 ^oC in air for 3 h and carbonized at 700 ^oC in 5% H_2/Ar atmosphere for 4 h to obtain Cu/C nanofibers. After that, the Cu/C nanofibers were soaked into the acetonitrile solution containing 15 mmol L^{-1} TCNQ for 20 min to obtained the CuTCNQ composite film.

Material characterization

Materials were characterized by scanning electron microscopy (SEM, FEI SIRION 200, Holland), powder X-ray diffraction (XRD, PANalytical B.V., Holland). UV-Vis absorbance was detected on a UV-2550 UV-Vis spectrophotometer (Shimadzu, Japan). Raman spectrometry was measured on Bruker VERTEX 70 equipment.

Electrochemical measurements

CuTCNQ composite films were cut into disks and used as working electrodes directly in CR2032 coin-type cells, while lithium metal pellets were applied as counter electrodes. The cells were assembled in an argon-filled glove box with a glass fiber membrane as the separator, 1.0 mol L^{-1}, 3 mol L^{-1}, 5 mol L^{-1} and 7 mol L^{-1} $LiClO_4$ in ethylene carbon (EC)/propylene carbonate (PC) (v/v = 1/1) as the electrolytes. The in-situ cell was assembled with a cuvette (size: 12.5(W)*12.5(L)*45(H)mm), CuTCNQ/CNFs cathode and Li foil anode fixing on two titanium foils (size: 6(W)*60(L) mm), respectively. Two electrodes are sealed in cuvette by a Teflon cover with 2 mL electrolyte and further sealed by sealing film. Galvanostatic charge-discharge was performed on a multi-channel battery testing system (Neware, China) at room temperature. The electrochemical impedance spectra (EIS) were performed on a PARSTAT 2273 potentiostat over the frequency ranging from 100 kHz to 0.1 Hz.

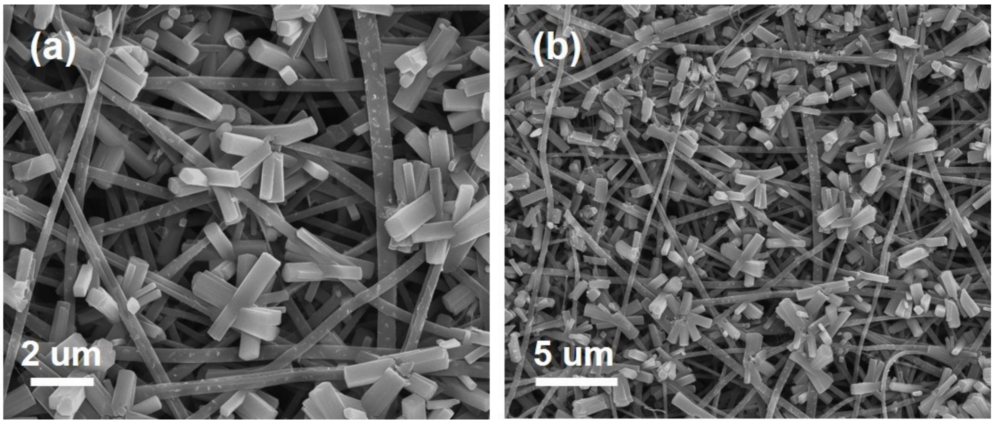

Fig. S1 (a, b) SEM images of CuTCNQ/CNFs composite. CuTCNQ is a flower-like nanorods connected by 3D carbon nanofiber conductive network.

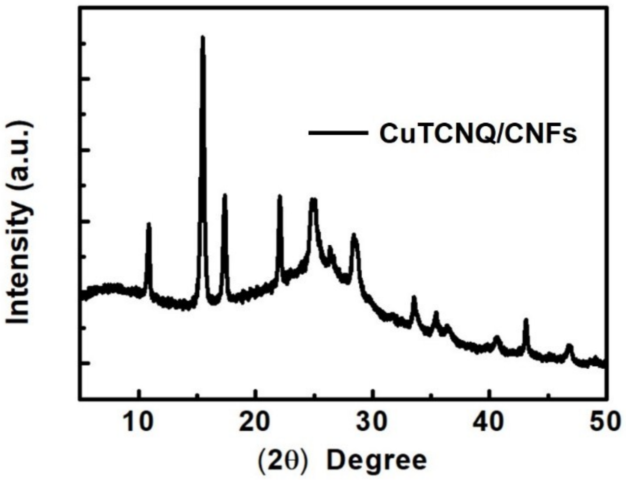

Fig. S2 XRD pattern of CuTCNQ and CNFs composite film. The CuTCNQ grown on the carbon nanofibers has a crystal structure of Phase I with a better electronic conductivity.

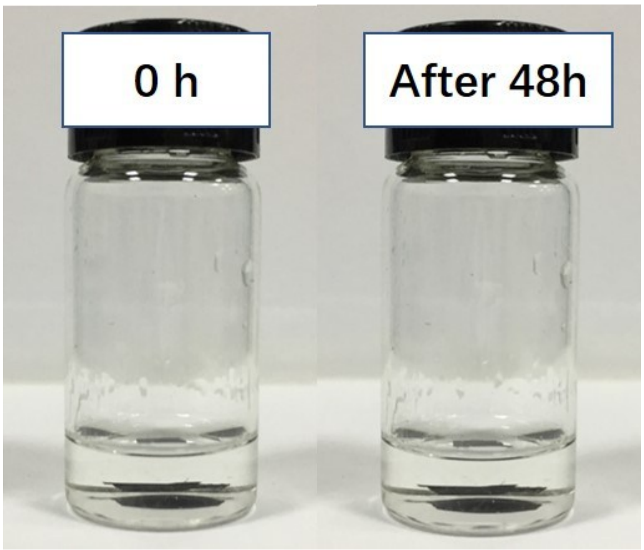

Fig. S3 Digital photos of CuTCNQ composite film soaking in 1M electrolyte.

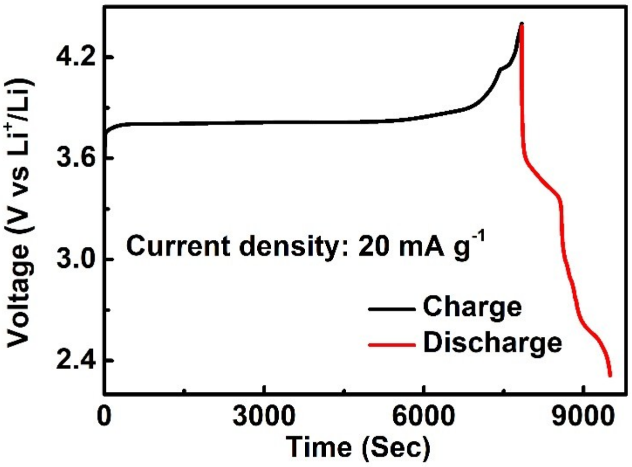

Fig. S4 Charge/discharge curve of the *in-situ* cell with 1 M $LiClO_4$ in EC/PC (v/v=1/1) electrolyte and the current density is 20 mA g^{-1}. During the discharge process, the voltage of cell dropped from 4.4 V to 2.0 V rapidly, which indicates lower discharge specific capacity is obtained.

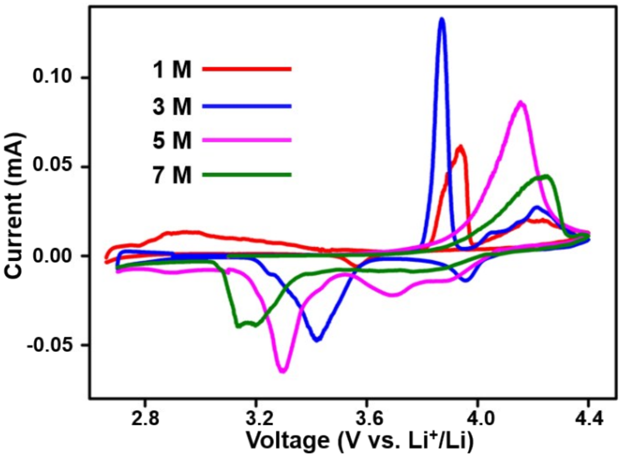

Fig. S5 CV curves for CuTCNQ/CNFs cathodes in 1, 3, 5 and 7 M electrolyte, respectively. The scan rate is 0.1 mV/s. The shift of oxidation peaks and reduction peaks for different concentration electrolyte indicating that the polarization is increased.

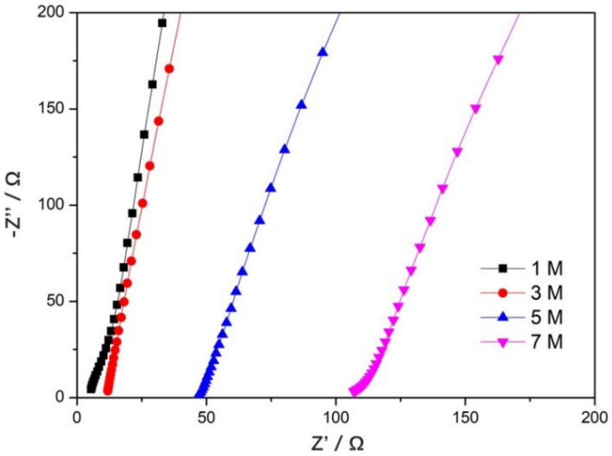

Fig. S6 Impedance spectra of the stain steel symmetric cells with different electrolyte concentration. The ionic conductivities are calculated based on the impedance spectra above. The resistance at the first intersection point is taken as *R*, while the thickness (*d*) and area (*A*) of separator are certain. Then, the ionic conductivity can be calculated based on $\sigma = d/(R \cdot A)$.

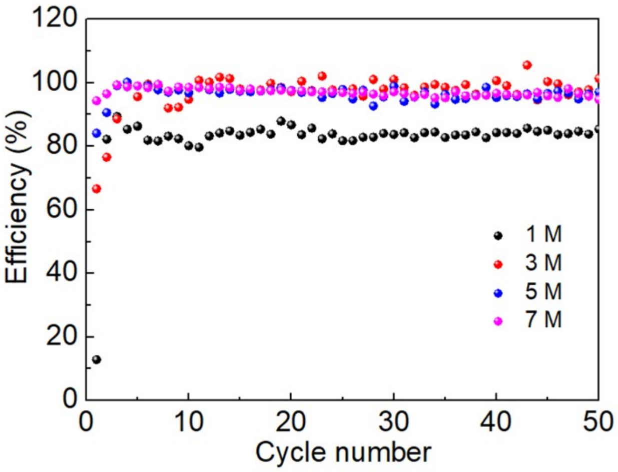

Fig. S7 Coulombic efficiency of Li/CuTCNQ cell in different electrolytes corresponding to Fig. 3(c).

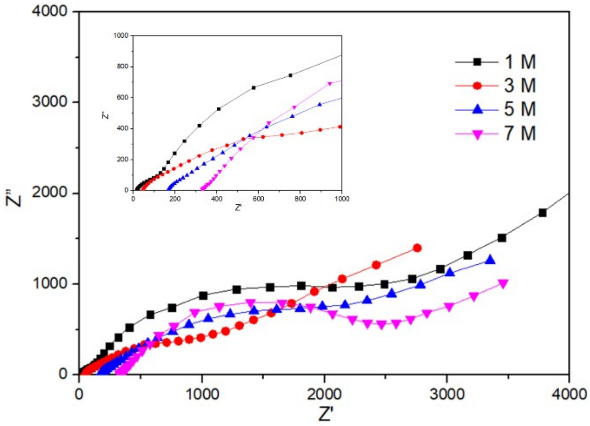

Fig. S8 Nyquist impedance spectra of CuTCNQ/Li cells in different electrolytes.

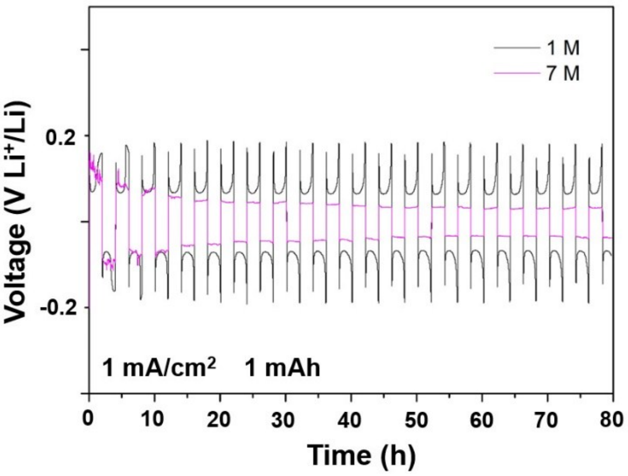

Fig. S9 Galvanostatic voltage-time curves for Li/Li symmetric cells with 1 and 7 M electrolyte.

(1) Charge Process:

$$Cu^+TCNQ^- + Li^+ClO_4^- - e^- \rightarrow TCNQ^0 + Cu^+ClO_4^- + Li^+$$

$$Cu^+ClO_4^- + Li^+ClO_4^- - e^- \rightarrow Cu^{2+}(ClO_4)_2^- + Li^+$$

(2) Discharge Process:

$$Cu^{2+}(ClO_4)_2^- + Li^+ + e^- \rightarrow Cu^+ClO_4^- + Li^+ClO_4^-$$

$$TCNQ^0 + Cu^+ClO_4^- + Li^+ + e^- \rightarrow Cu^+TCNQ^- + Li^+ClO_4^-$$

$$Cu^+TCNQ^- + Li^+ + e^- \rightarrow Li^+[Cu^+(TCNQ)^{2-}]$$

Scheme S1 Redox reaction equations of CuTCNQ as cathode for LIBs.